# Wind Turbine Fault Detection Using Counter-Based Residual Thresholding ⋆

**Ahmet Arda Ozdemir, Peter Seiler, and Gary J. Balas** *

* *Department of Aerospace Engineering and Mechanics, University of Minnesota, Minneapolis, MN 55455, USA (e-mail: arda@aem.umn.edu, seiler@aem.umn.edu, balas@aem.umn.edu)*

**Abstract:** Up-down counters are commonly used in the aerospace industry for fault detection thresholding. This paper applies the up-down counter technique to detect wind turbine faults. The thresholding problem involves a tradeoff between false alarms and missed detections. Counter based thresholding can detect smaller faults with higher probability and lower false alarms than is possible using simple constant thresholds. This improvement is achieved by effectively introducing dynamics into the thresholding logic as opposed to decisioning based on a single time step. Up down counters are applied to the development of a fault detection system for a commercial sized 4.8MW wind turbine. Realistic fault scenarios in the sensing, actuation and drivetrain subsystems are considered. It is seen that most faults can be detected with fast detection times and minimal false alarms without implementation of more complex filtering and detection techniques on residuals.

*Keywords:* Fault detection, Counters, Threshold selection, Wind Turbine

## 1. INTRODUCTION

Wind energy is a rapidly growing renewable energy source as its cost per unit is reaching competitive levels. Maintenance and repair costs constitute an important portion of the operating costs of a typical wind turbine. These costs are more significant for offshore wind turbines which are located further from the maintenance centers. In addition, offshore wind turbines in general have lower availability rates than their onshore counterparts due to the longer repair times.

Fault detection and isolation (FDI) algorithms can be used to detect the irregularities in the sensing and actuation subsystems of the wind turbine and accommodate these faults when possible. In addition, FDI systems can also be used for detection of the precursors of some critical failures, which may otherwise result in a high cost breakdown in the future. These benefits of the FDI systems can significantly reduce the downtime and repair costs of the wind turbine over its lifetime.

The fault detection problem usually comprises a method to compute residuals and a process to declare faults based on the residuals. It is desired that the generated residual be a good representation of the fault of interest while being insensitive to process and measurement noises. Generation of residuals depends on the information available about the system. If a sufficiently accurate model of the system is available, model based methods can be used to estimate system states and outputs. Donders (2002) applied Kalman Filter and Interacting Multiple-Model estimators to the wind turbine FDI problem. $H_\infty/H_-$ techniques for observer design were used by Wei and Verhaegen (2008) and Szaszi et al. (2002). Another method of obtaining residuals is to compare the redundant information about the system if the system has some physical redundancy built in it. See Gertler (1998), Isermann (2005), and Ding (2008) for a detailed treatment of model based and model-free fault detection methods.

A common method used for decision making in fault detection algorithms is thresholding. That is, a fault is declared if the residual exceeds a certain threshold. See Gertler (1998), Emami-Naeini et al. (1988) for applications of fixed thresholding and see Stoustrup et al. (2003) for time varying thresholding. Another method used for decisioning is up-down counters which are also known as leaky bucket counters in the communications and software literature. See Logothetis and Trivedi (1994) and Butto et al. (1991) for the applications of leaky bucket counters in the communications literature. These counters are also commonly used in aerospace industry for fault detection purposes. Gertler (1998) used a special case of the up-down counters for fault detection where the up and down-counts at each time step are simply set equal to one. The operation of these counters is explained in detail in Section 3.3.

This paper develops a fault detection and isolation system for a typical commercial wind turbine. Faults are considered in the pitch actuators and sensors, rotor speed and

⋆ This work was supported by the University of Minnesota Institute on the Environment, IREE Grant No. RS-0039-09, the US Department of Energy Contract No. DE-EE0002980 and the US National Science Foundation under Grant No. NSF-CNS-0931931. Any opinions, findings, and conclusions or recommendations expressed in this material are those of the author(s) and do not necessarily reflect the views of the University of Minnesota, Department of Energy or National Science Foundation.

generator speed sensors as well as system faults in the drivetrain and generator. Both model based and physical redundancy based residuals are used. Up-down counters are used for decisioning on each residual.

The paper has the following structure: Section 2 describes the wind turbine model used in this paper and explains the faults that are considered. Section 3 explains the design of the FDI system in detail. The results are presented in Section 4. Conclusions are presented in Section 5.

## 2. WIND TURBINE MODEL AND PROBLEM FORMULATION

The wind turbine model and problem considered in this paper is based on the work presented in Odgaard et al. (2009). The modeled turbine is a variable speed, three bladed horizontal axis wind turbine with a rated power of 4.8 MW. A brief overview of the problem formulation is presented in this section.

### *2.1 Aerodynamics and Pitch System Model*

The captured power is approximately given by:

$$P_r = \tau_{aero}\omega_r = \frac{1}{2}\rho A v^3 C_p(\lambda,\beta) \tag{1}$$

where $\tau_{aero}$ (N) is the aerodynamic torque, $\omega_r$ (rad/s) is the rotor speed, $\rho$ $(kg/m^3)$ is the air density, $A$ $(m^2)$ is the area swept by the rotor, $v$ (m/s) is the wind speed. $C_p$ (unitless) is the power coefficient which represents how much of the power available in wind is captured. $C_p$ is a function of blade pitch angle $\beta$ (deg) and tip speed ratio $\lambda$ (unitless) where $\lambda$ is defined as:

$$\lambda = \frac{\omega_r R}{v} \tag{2}$$

$R$ (m) is the rotor radius. From Equation (1), it is seen that the aerodynamic torque can be written as:

$$\tau_{aero} = \frac{\rho A v^3 C_p(\lambda,\beta)}{2\omega_r} \tag{3}$$

The pitch actuators on the system are represented by a second-order transfer function $G_{act}(s)$:

$$\frac{\beta(s)}{\beta_{ref}(s)} = G_{act}(s) = \frac{\omega_n^2}{s^2 + 2\zeta\omega_n s + \omega_n^2} \tag{4}$$

The nominal values of $\zeta$ and $\omega_n$ are 0.6 and 11.11 respectively.

### *2.2 Drivetrain and Generator Model*

Drivetrain flexibility is modeled by a two mass model:

$$\begin{bmatrix}\dot{\omega_r}\\ \dot{\omega_g}\\ \dot{\theta}_\Delta\end{bmatrix} = A_{dt}\begin{bmatrix}\omega_r\\ \omega_g\\ \theta_\Delta\end{bmatrix} + \begin{bmatrix}-1/J_r & 0\\ 0 & 1/J_g\\ 0 & 0\end{bmatrix}\begin{bmatrix}\tau_{aero}\\ \tau_g\end{bmatrix} \tag{5}$$

$$A_{dt} = \begin{bmatrix}\frac{-(B_{dt}+B_r)}{J_r} & \frac{B_{dt}}{N_g J_r} & \frac{-K_{dt}}{J_r}\\ \frac{\eta_{dt}B_{dt}}{N_g J_g} & \frac{-\eta_{dt}B_{dt} - B_g N_g^2}{N_g^2 J_g} & \frac{\eta_{dt}K_{dt}}{N_g J_g}\\ 1 & -\frac{1}{N_g} & 0\end{bmatrix} \tag{6}$$

where $\omega_r$ is the rotor speed, $\omega_g$ is the generator speed, $\theta_\Delta$ is the drivetrain torsion, $J_r$ and $J_g$ are the rotor and generator inertia, $B_r$ and $B_g$ are the viscous damping of the rotor and generator, $B_{dt}$ and $K_{dt}$ are the damping and stiffness coefficients of the drivetrain flexibility, and $N_g$ is the gearbox ratio.

The dynamics of the generator are modeled with a first-order transfer function:

$$\frac{\tau_g(s)}{\tau_{g,ref}(s)} = G_{gen}(s) = \frac{\alpha_g}{s+\alpha_g} \tag{7}$$

The nominal value of $\alpha_g = 50$. See Odgaard et al. (2009) for the numeric values of the constants specified in this section.

### *2.3 Control Systems*

The control system of the turbine includes two separate controllers for Region 2 and Region 3 operation.

When the turbine is in Region 2 or power optimization mode, blades are pitched to $\beta_{opt} = 0°$. Generator torque is set as:

$$\tau_{g,ref} = \frac{1}{2}\rho A R^3 \frac{C_{p_{max}}}{\lambda_{opt}^3}\omega_r^2 \tag{8}$$

This control law simply drives the rotor speed to the optimal tip speed ratio ($\lambda_{opt}$) in steady state, which yields the optimal power coefficient $C_{p_{max}} = C_p(\beta_{opt}, \lambda_{opt})$. For the details of this control law, see Johnson et al. (2006).

If the turbine is operating in Region 3, a discrete PI controller generates blade pitch commands to maintain the rated rotor speed. The generator torque is set as:

$$\tau_{g,ref} = \frac{P_{rated}}{\omega_g} \tag{9}$$

such that the generator captures the rated power of the turbine. Note that this simple control scheme does not include individual pitch control (IPC) for turbine structural load reduction. The FDI system presented in this paper is not specific to this control scheme and can be implemented on any IPC control law without any modifications.

### *2.4 Sensor Configuration*

Typically, wind turbines are built with sensor configurations that involve some physical redundancy for fault tolerant operation. The available sensors on the model are listed in Table 1. Subscripts _m1 and _m2 represent redundant measurements of the quantities. In addition to the measurements listed in Table 1, it is assumed that the digital controller commands are also available for the FDI system. The sampling time of the sensors is assumed to be $T_s = 0.01$ seconds.

Table 1. Sensor Configuation of Wind Turbine

| Sensor | Symbols | Noise ($\mu$, $\sigma^2$) |
|---|---|---|
| Rotor Speed | $\omega_{r\_m1}$, $\omega_{r\_m2}$ (rad/s) | (0, 0.025) |
| Generator Speed | $\omega_{g\_m1}$, $\omega_{g\_m2}$ (rad/s) | (0, 0.050) |
| Generator Torque | $\tau_{g\_m}$ (Nm) | (0, 90) |
| Generator Power | $P_{g\_m}$ (W) | (0, 1000) |
| i-th Blade Pitch Angle | $\beta_{i\_m1}$, $\beta_{i\_m2}$ (deg) | (0, 0.200) |
| Wind Speed | $v_m$ (m/s) | (1.5, 0.500) |

The noises acting on each sensor are assumed to be Gaussian white noise. The mean values ($\mu$) and variances

($\sigma^2$) of the sensor noises are given in Table 1. The wind speed sensor is considered to have low accuracy and it requires calibration frequently. In addition, note that the standard deviation of the rotor speed measurement is $\sigma \approx 0.1581$. This corresponds to approximately 10% of the rated rotor speed of 1.7 rad/s. The large noise on this measurement was an issue in our baseline designs.

### *2.5 Fault Modeling and Detection Requirements*

The sensor faults considered in this paper are listed in Table 2. It is required that these faults (Faults 1-5) are detected in $10T_s$, i.e. 10 sampling periods of the sensors.

Table 2. List of Sensor Faults

| Fault No | Fault | Description |
|---|---|---|
| 1 | $\beta_{1\_m1}$=5 deg | Pitch Sensor Stuck |
| 2 | $\beta_{2\_m2}$=1.2$\beta_{2_m2}$ | Pitch Sensor Scale Factor |
| 3 | $\beta_{3\_m1}$=10 deg | Pitch Sensor Stuck |
| 4 | $\omega_{r\_m1}$=1.4 rad/s | Rotor Speed Sensor Stuck |
| 5 | $\omega_{r\_m2}$=1.1$\omega_{r_m2}$ $\omega_{g\_m2}$=0.9$\omega_{g_m2}$ | Simultaneous Rotor Speed and Gen. Speed Sensor Scale Factor |

Two fault scenarios are considered for pitch actuator faults (Faults 6 and 7). Fault 6 is a hydraulic failure in the pitch actuator 2 which involves an abrupt change in pitch actuator model parameters $\zeta$ and $\omega_n$. The second scenario, Fault 7, involves increased air content in the actuator oil which manifests itself with slower actuator response over time. This fault is modeled as a slow, time varying change in actuator parameters $\zeta$ and $\omega_n$. Bode plots of the nominal and faulty actuator models are presented in Figure 1. Detection time requirements for these actuator faults are given as $8T_s$, and $600T_s$ respectively.

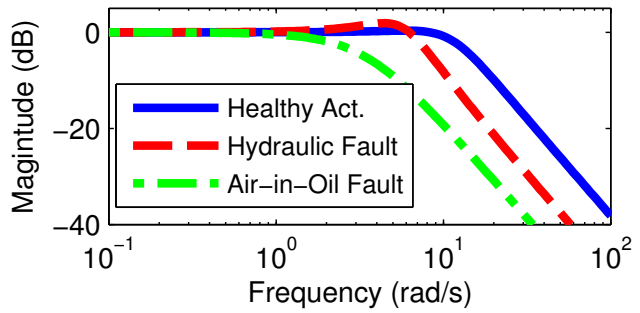


Fig. 1. Bode Plots for Healthy and Faulty Actuator Models

In addition, two system level faults are considered (Faults 8 and 9). The first system level fault, Fault 8, involves an offset in the inner control loop of the generator. It results in a bias in the generator torque $\tau_g = \tau_g + 100$ (Nm). The second system level fault considered is the increased friction in the drivetrain (Fault 9). This fault typically develops slowly over time and results in increased vibrations in the drivetrain. This fault is modeled with a 5% change in the drivetrain efficiency $\eta_{dt}$. Fault 8 needs to be detected in $5T_s$ and there are no time restrictions for the detection of Fault 9. A list of the actuator and system level faults are given in Table 3.

In addition to the detection time constraints, it is required that the false alarm rate be less than 1 in $10^5$ time steps. It is also expected that the false alarms are cleared in three time steps.

Table 3. List of Actuator and System Faults

| Fault No | Description |
|---|---|
| 6 | Pitch Actuator 2 Hydraulic Failure |
| 7 | Pitch Actuator 3 Air in Oil Failure |
| 8 | Generator Inner Control Loop Failure |
| 9 | Increased Drivetrain Friction due to Wear |

## 3. FAULT DETECTION SYSTEM

Most FDI systems involve a method to generate residuals from system measurements and a thresholding logic to declare faults based on these residuals. Section 3.1 provides an overview of the residual generation methods used in this paper. Section 3.3 describes the up-down counter thresholding logic.

### *3.1 Residual Generation Methods*

*Physical Redundancy Based* A residual $r$ can be generated by direct comparison of the physically redundant measurements of the same quantity $m_1$ and $m_2$:

$$r = m_1 - m_2 \tag{10}$$

$r$ represents the noise on the sensors if the system is healthy. If one of the sensors is faulty, the residual carries the fault and the noise. The disadvantage of this approach is that the residual typically carries a larger variance than the individual noises, given by equation:

$$Var[r] = Var[m_1] + Var[m_2] + 2Cov[m_1, m_2] \tag{11}$$

Generally it is assumed that the measurement noises from redundant sensors are independent and identically distributed. For this case, the variance of the residual is twice as large as the sensor noise variance, i.e.

$$Var[r] = 2Var[m_1] = 2Var[m_2] \tag{12}$$

*Parity Equations* An ideal response of a system can be obtained if a reasonably accurate model of the system and its inputs are available. Typically available transfer functions are discretized for implementation on digital processors and ideal system responses are calculated. Various residuals can be generated by comparing this ideal response with measurements from the physical system.

*Kalman Filter* The well known Kalman Filter yields the optimal minimum-variance state estimate of a linear system subject to Gaussian noise. It is desired to obtain low noise estimates of the rotor and generator speed measurements. Hence an estimate of the drivetrain states are obtained using a Kalman Filter based on the drivetrain system model Eq. (5). Filter structure is shown in Figure 2. The Kalman Filter inputs are the average of the rotor and generator speed measurements, and the generator torque measurement. In case of a fault in rotor or generator speed measurements, only the healthy measurements are fed to the Kalman filter instead of the average of the redundant measurements. The filter outputs are used for identification of the faulty rotor and generator speed measurements.

### *3.2 Fault Residuals*

The FDI system uses physical redundancy based residuals for pitch angle sensors. This residual is sufficient for

Fig. 2. Kalman Filter for Drivetrain System

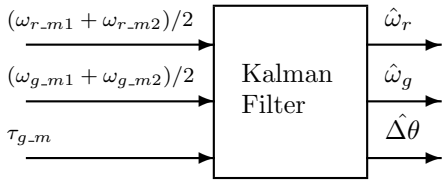


fault detection but additional information is required for diagnosing the faulty sensor. Ideal pitch responses are obtained via parity equations and controller pitch commands. Comparison of ideal pitch response against each measurement yields two extra residuals for fault diagnosis. These residuals are not affected by other faults in the turbine and no specific fault isolation measures are taken.

Fault residuals for three pitch actuators are obtained by comparing ideal pitch response against pitch angle measurements. If both sensors are healthy, the average of the two measurements is taken for comparison. In case there is a pitch sensor fault, only the healthy measurement is used. A sixth-order elliptical filter with $1dB$ pass-band ripple has been used on these residuals due to high noise levels. An elliptical filter is chosen due to its fast rolloff characteristics at its cutoff frequency. Actuator faults are mainly observed in the mid-frequency range. Therefore less than unity gain at DC frequency achieved by elliptical filters is not detrimental for FDI performance. The residual carries higher noise when one of the pitch sensors are faulty. Fault flagging system should be designed to satisfy FDI system requirements under this condition.

Rotor and generator speed sensor faults are observed through dual measurements of each quantity. The difference between the drivetrain Kalman filter outputs and each measurement is used for fault diagnosis. The rotor speed measurements have a low signal-to-noise ratio. Hence the rotor speed rotor speed residuals are averaged over 40 time steps to reduce the variance of the Gaussian white noise in the steady state. This corresponds to the digital filter $F_{\omega_r}(z)$:

$$F_{\omega_r}(z) = \frac{1}{40}\frac{z^{40} + z^{39} + ... + z^2 + z^1 + 1}{z^{40}} \qquad (13)$$

Generator system faults are detected using controller generator torque commands and parity equations for the generator system. This residual is not affected by faults other than generator system fault.

The drivetrain system fault could not be detected and is discussed further in Section 4.

### *3.3 Up-Down Counters*

Discrete time up-down counters are used for the decision making process on residuals generated for each fault in this paper. Counters involve six parameters in the most general case: up-count amount $+U$, down-count amount $-D$, up-counting threshold $Tol_1$, fault declaration threshold $Tol_2$, counter lowerbound $LB$, and counter upperbound $UB$. At each time step an up-count is triggered if the residual exceeds $Tol_1$ otherwise the counter counts down by $-D$. A fault is declared if the value of the counter exceeds $Tol_2$. The structure of the up-down counter is shown in Figure 3.

Fig. 3. Up/Down Counter Structure

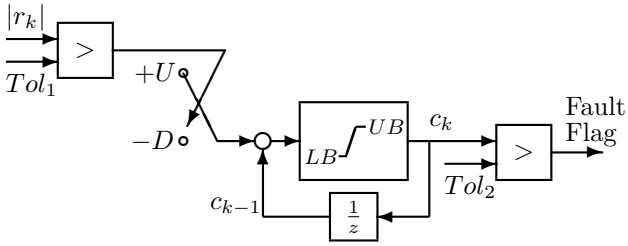


The use of up-down counters differs from straightforward thresholding in two ways. First, the decision to declare a fault involves discrete-time dynamics and is not simply a function of the current value of the residual. Therefore the extra time specified by the detection time constraints can be utilized. Second, up-count and down-count parameters $+U$ and $-D$ introduce a penalty on the residual exceeding the $Tol_1$ threshold. These features enable the designer to use a lower $Tol_1$ compared to typical thresholding and to detect smaller faults with higher detection rates, without increasing false-alarm rates. Note that typical threshold schemes are just a special case of an up-down counter. In particular, if $U > (UB - LB)$ and $-D = -U$ then the up-down counter will declare a fault if the residual exceeds $Tol_1$ for one time step.

Fixed counter parameters are used in this work. All parameters except $Tol_1$ are chosen as integers for ease of design and implementation. It can be seen that $+U$, $-D$, $Tol_2$, $LB$, and $UB$ can be scaled together without any effect. Hence, $-D = -1$ is chosen to eliminate one parameter from the counter design. As a starting point, $LB$=0 and $UB$=255 are chosen so that the counter can be implemented using 8-bit unsigned integers. This choice will significantly reduce the memory and computational costs required by the implementation if the FDI system has many up-down counters. This leaves three parameters to choose for up-down counter: $Tol_1$, $+U$, and $Tol_2$. These parameters are chosen according to the nature of the fault of interest and the noise on the residual.

The first stage of the counter design involves determining $Tol_1$. This is a similar process to the selection of a fixed threshold. Assuming a statistical distribution for the noise on residual, $Tol_1$ is chosen to result in a predetermined false up-count rate $P_{up\_false}$. $Tol_1$ reflects the sensitivity of the fault detection system and it involves a tradeoff between false alarms and missed detections. If the fault of interest is significantly larger than the noise on the data, a larger $Tol_1$ can be chosen to minimize the false alarms. On the other hand, if the noise level is high compared to the fault, a lower $Tol_1$ must be chosen at the expense of higher false alarms to avoid a missed detection.

In general, it is desired to have faster up-counts than down-counts. This basically relies on the fact that commonly $P_{up\_false}$ is significantly smaller than the up-count probability in existence of the fault, i.e. $P_{up\_fault}$. Typically, harder to detect faults require higher $+U$ values to avoid missed detections. For instance, the pitch actuator faults can be most easily distinguished at mid-frequency range. These faults cannot be detected unless there are pitch commands in this frequency range and counters can count down often during fault. On the contrary, note that the

up-counts $+U$ must be limited for clearing the false alarms quickly.

The last stage of the design involves obtaining $Tol_2$. As a starting point, $Tol_2$ is chosen as $+U^n$ where n is found by using false alarm constraint $P_{faconst}$:

$$n = log_{P_{up\_false}}(P_{faconst}) \tag{14}$$

then $+U^n$ is rounded to the nearest integer towards infinity and set as $Tol_2$. If the $P_{up\_false}$ is small enough, this equation approximately ensures that the false alarm requirements are met since it should take about n steps of false up-counting to exceed the $Tol_2$ in case of healthy operation. The final value of $Tol_2$ for each fault is set after some iterations.

Introducing discrete time dynamics into the fault detection algorithm with up-down counters can be compared with combination of linear filters and fixed thresholding. Up-down counters can be implemented with small memory and computational requirements. Up-down counters also offer good rejection of single event upsets (e.g. due to corrupted memory) by having finite up-counts. On the other hand, design of simple linear filters are more straightforward. Linear filters provide an intuitive way for frequency based noise attenuation. This paper uses a combination of these two methods.

## 4. SIMULATION RESULTS

The designed fault detection system is simulated 100 times with different randomly generated noise sequences on each sensor. The wind disturbance used is given by Odgaard et al. (2009) and shown in Figure 4. This section summarizes the results of these simulations.

Fig. 4. Wind Disturbance and Turbine Operating Zones

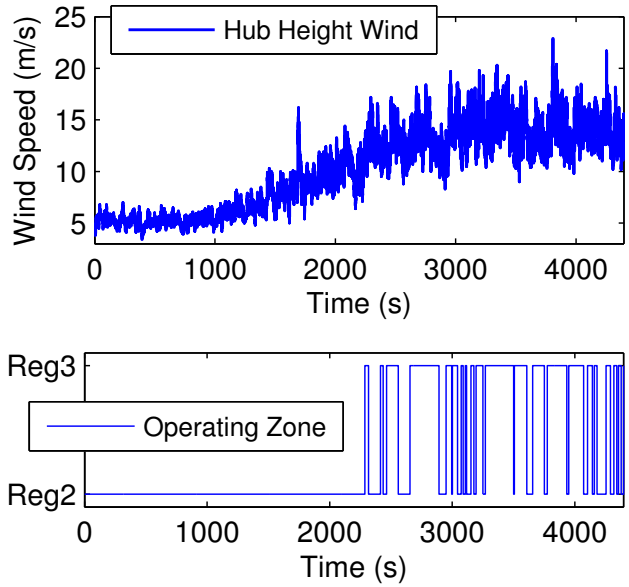


Table 4 lists the average fault detection times, false alarm rates, missed detections, and the average time required for clearing false alarms for each fault. False alarm rate is defined as the number of false alarms per digital processor time step $T_s = 0.01$ (s). Entries in the table that satisfy the design specifications are marked in green and the failed specifications are marked in red. It is seen in Table 4 that false alarm rate constraints are satisfied for all of the faults. False alarm clearance time requirements are not satisfied for Faults 4 and 5. A pitch sensor fault (Fault 2), faults related to the rotor speed sensors (Faults 4 and 5), and pitch actuator faults (Faults 6 and 7) required more time than the specified time limits for detection.

Table 4. Simulation Results

| F. No | Det. Time | FA Rate | Missed | FA Clear. Time |
|---|---|---|---|---|
| 1 | 3 $T_s$ | $0.091/10^5$ | 0 | 2.9 $T_s$ |
| 2 | 819.4 $T_s$ | $0.046/10^5$ | 0 | 2.3 $T_s$ |
| 3 | 3 $T_s$ | $0.046/10^5$ | 0 | 2.4 $T_s$ |
| 4 | 12.4 $T_s$ | $0.068/10^5$ | 0 | 18.8 $T_s$ |
| 5 | 187.4 $T_s$ $\omega_{r\_m2}$<br>2 $T_s$ $\omega_{g\_m1}$ | $0.159/10^5$<br>$0/10^5$ | 0<br>0 | 17.5 $T_s$<br>0 $T_s$ |
| 6 | 5050 $T_s$ | $0.182/10^5$ | 0 | 3.9 $T_s$ |
| 7 | 1573 $T_s$ | $0.022/10^5$ | 0 | 3.2 $T_s$ |
| 8 | 1 $T_s$ | $0/10^5$ | 0 | 0 $T_s$ |
| 9 | N/A | N/A | 100 | N/A |

The late detection of Fault 2 is due to the turbine operating conditions for the duration of the fault 2300-2400 (s). The scale factor on the pitch angle can only be detected if the blade pitch angle is large enough to distinguish the fault from the noise. The wind speed is close to the rated wind speed in this time interval. The turbine is operating in Region 3 and generating nonzero pitch commands only during 2300-2320 (s) interval. The fault is detected only for a short duration when the pitch commands reach about 5 degrees around $t = 2308$ (s).

The rotor speed sensor faults (Faults 4 and 5) are hard to detect due to the large noise on the rotor speed sensors. Fault 5 corresponds to a measurement error of about 0.06 rad/s whereas the standard deviation of the measurement noise is 0.1585 rad/s. The residuals for the rotor speed sensors before and after filtering are given in Figure 5. Before filtering, the fault occurring at $t = 1000$ (s) is indistinguishable from the sensor noise. The high-order low-pass filtering applied to the fault residual results in a slow detection of faults in these sensors. The failed false alarm clearance time constraints are also due to this low-pass filtering since it takes longer for residual to fall below the upcounting tolerance once it is exceeded.

Fig. 5. Rotor Speed Sensor Residual

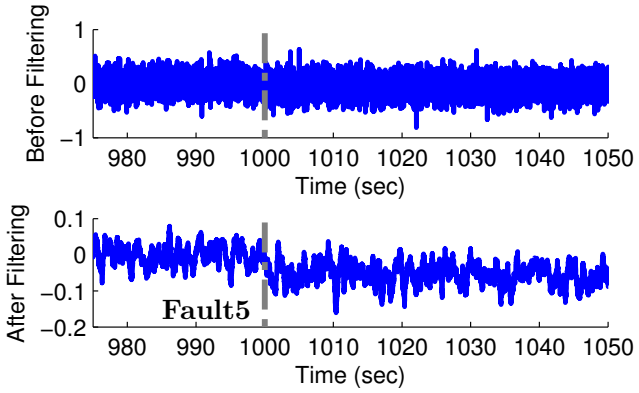


The main reason behind the slow detection of the actuator faults (Faults 6 and 7) is due to the nature of actuator

failures. From Figure 1 it can be seen that the healthy and faulty actuator models show similar behavior at low frequencies and roll off at high frequencies. Therefore, pitch actuator faults can only be observed if the pitch commands include components at mid frequency range where the faulty and nominal actuator models have different frequency responses. This requires the turbine to be in Region 3 for the successful detection. The slow detection of the air-in-oil fault (Fault 7) is due to turbine operating close to Region 2 when the fault is initiated. The controller is generating pitch commands close to zero degrees and slight changes in the model are difficult to detect. The air-in-oil fault has an additional 30° of phase at 1 rad/sec compared to the nominal system. It might be possible to design a filter for the air-in-oil fault based on the phase change. The fault detection system satisfies the detection time requirements for Fault 6 if the detection time is calculated from the time turbine switches to Region 3 operation.

The behavior of the up-down counters for the 2nd blade pitch actuator fault (Fault 6) is shown in the top plot of Figure 6. As discussed, pitch actuator faults can only be observed under certain conditions hence the counter counts down occasionally during the fault. Therefore large up-count values $+U$ are used for this fault to avoid removing the fault flag too early under faulty operation. The counter for the generator system fault (Fault 8) is shown in the bottom plot of Figure 6. The generator system fault of interest is significantly larger than the noise on the residual thus it is easy to detect. Small up-counts with lower residual tolerances are sufficient in this case since it is unlikely that the counter will count down due to noise under faulty operation. From Table 4 it is seen that this fault has substantially faster detection times and lower false alarm rates compared to the other faults.

Fig. 6. Up-down Counter Values During Faults

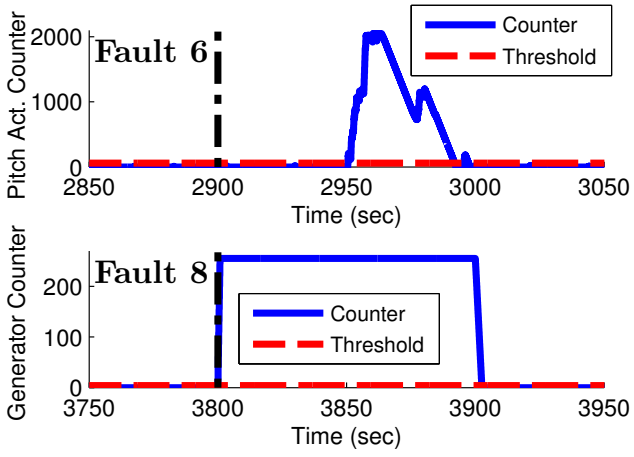


The detection of the drivetrain fault (Fault 9) is challenging for model-based approaches. Fault 9 creates only a small change in the drivetrain dynamics. The effect of this fault cannot be distinguished from the effect of unknown aerodynamic torque disturbance based on rotor and generator speed measurements. Estimation of the aerodynamic torque through the $C_p - \beta - \lambda$ mapping of the turbine typically carries about 2-3% uncertainty and depends on unreliable wind speed measurements. Therefore it is difficult to estimate a 5% change in the drivetrain efficiency based on estimation of the aerodynamic torque.

## 5. CONCLUSIONS

This paper considered the use of the up-down counters for wind turbine fault detection and isolation. The parameters of the counters were selected based on physical insight of each fault of interest. It is seen that faults of lower magnitude can be detected without increasing the false alarm rates. Future work will focus on the development of the relationships between the statistical properties of the residual, detection and false alarm rates, and fault magnitude.

## REFERENCES


Butto, M., Cavallero, E., and Tonietti, A. (1991). Effectiveness of the 'leaky bucket' policing mechanism in atm networks. *Selected Areas in Communications, IEEE Journal on*, 9(3), 335 –342.

Ding, S.X. (2008). *Model-based Fault Diagnosis Techniques: Design Schemes, Algorithms, and Tools*. Springer, 1st edition.

Donders, S. (2002). *Fault Detection and Identification for Wind Turbine Systems: a closed-loop analysis*. Master's thesis, University of Twente.

Emami-Naeini, A., Akhter, M., and Rock, S. (1988). Effect of model uncertainty on failure detection: the threshold selector. *Automatic Control, IEEE Transactions on*, 33(12), 1106–1115.

Gertler, J.J. (1998). *Fault detection and diagnosis in engineering systems*. Marcel Dekker, 1st edition.

Isermann, R. (2005). *Fault-diagnosis systems: an introduction from fault detection to fault tolerance*. Springer, 1st edition.

Johnson, K., Pao, L., Balas, M., and Fingersh, L. (2006). Control of variable-speed wind turbines: standard and adaptive techniques for maximizing energy capture. *Control Systems Magazine, IEEE*, 26(3), 70 – 81.

Logothetis, D. and Trivedi, K. (1994). Transient analysis of the leaky bucket rate control scheme under poisson and on-off sources. In *INFOCOM '94. Networking for Global Communications., 13th Proceedings IEEE*, 490 – 497 vol.2.

Odgaard, P.F., Stoustrup, J., and Kinnaert, M. (2009). Fault tolerant control of wind turbines - a benchmark model. In *Proceedings of Fault Detection, Supervision and Safety of Technical Processes*.

Stoustrup, J., Niemann, H., and la Cour-Harbo, A. (2003). Optimal threshold functions for fault detection and isolation. In *American Control Conference, 2003. Proceedings of the 2003*, volume 2, 1782–1787.

Szaszi, I., Kulcsar, B., Balas, G., and Bokor, J. (2002). Design of fdi filter for an aircraft control system. In *American Control Conference, 2002. Proceedings of the 2002*, volume 5, 4232–4237.

Wei, X. and Verhaegen, M. (2008). Fault detection of large scale wind turbine systems: A mixed $H_\infty/H_-$ index observer approach. In *Control and Automation, 2008 16th Mediterranean Conference on*, 1675–1680.